Hindawi Publishing Corporation
X-Ray Optics and Instrumentation
Volume 2010, Article ID 109740, 19 pages
doi:10.1155/2010/109740

*Review Article*

# Focusing X-Ray Optics for Astronomy

**Paul Gorenstein**

*High Energy Astrophysics Division, Harvard-Smithsonian Center for Astrophysics, 60 Garden Street, MS-4, Cambridge, MA 02138, USA*

Correspondence should be addressed to Paul Gorenstein, pgorenstein@cfa.harvard.edu

Received 28 February 2010; Accepted 12 October 2010

Academic Editor: Stephen L. O'Dell



Focusing X-ray telescopes have been the most important factor in X-ray astronomy's ascent to equality with optical and radio astronomy. They are the prime tool for studying thermal emission from very high temperature regions, non-thermal synchrotron radiation from very high energy particles in magnetic fields and inverse Compton scattering of lower energy photons into the X-ray band. Four missions with focusing grazing incidence X-ray telescopes based upon the Wolter 1 geometry are currently operating in space within the 0.2 to 10 keV band. Two observatory class missions have been operating since 1999 with both imaging capability and high resolution dispersive spectrometers. They are NASA's Chandra X-ray Observatory, which has an angular resolution of 0.5 arc seconds and an area of 0.1 $m^2$ and ESA's XMM-Newton which has 3 co-aligned telescopes with a combined effective area of 0.43 $m^2$ and a resolution of 15 arc seconds. The two others are Japan's Suzaku with lower spatial resolution and non-dispersive spectroscopy and the XRT of Swift which observes and precisely positions the X-ray afterglows of gamma-ray bursts. New missions include focusing telescopes with much broader bandwidth and telescopes that will perform a new sky survey. NASA, ESA, and Japan's space agency are collaborating in developing an observatory with very large effective area for very high energy resolution dispersive and non-dispersive spectroscopy. New technologies are required to improve upon the angular resolution of Chandra. Adaptive optics should provide modest improvement. However, orders of magnitude improvement can be achieved only by employing physical optics. Transmitting diffractive-refractive lenses are capable theoretically of achieving sub-milli arc second resolution. X-ray interferometry could in theory achieve 0.1 micro arc second resolution, which is sufficient to image the event horizon of super massive black holes at the center of nearby active galaxies. However, the physical optics systems have focal lengths in the range $10^3$ to $10^4$ km and cannot be realized until the technology for accurately positioned long distance formation flying between optics and detector is developed.

## 1. Introduction

Over the past decade focusing X-ray telescopes have had a very prominent role in astronomy, cosmology, and in positioning astrophysics at the frontier of fundamental physics. Currently (2010), four focusing X-ray telescopes are in space. The most notable are aboard two complementary missions. They are NASA's Chandra X-ray Observatory which has very high angular resolution and moderately high throughput, and the European Space Agency's XMM-Newton, which has high throughput and moderate angular resolution. There is also a Japanese led mission called Suzaku and the Swift mission, whose payload includes an X-ray telescope (XRT). NASA and ESA plus JAXA, the Japanese space agency, are collaborating on the development of the next major X-ray astronomy observatory mission, named the International X-Ray Observatory (IXO), whose telescope will have far more throughput than any other to date and whose X-ray spectrometers will be far more powerful in every respect than any currently in space. Information about all current and past X-ray astronomy missions in which NASA has participated is available at the website http://heasarc.nasa.gov/docs/observatories.html.

This paper provides background and general information about X-ray optics for astronomy and is an introduction to the more detailed descriptions of specific topics that appear in other articles in this issue.

The energy band where focusing X-ray telescopes currently are operating is 0.2 to 10 keV. These limits are not strict. Below the low-energy limit the interstellar medium is

Table 1: Various types of optics for X-ray telescopes.

| Type | Best angular resolution (half power diam.) | Energy band | Status | Astronomical applications |
|---|---|---|---|---|
| Grazing incidence reflection | 0.5 arcsec (actual) | 0.15–10 keV | Currently operating*** | Imaging and spectroscopy of all type objects |
| Grazing incidence reflection with ML coatings** | 0.4 to 1 arcmin | 5–>80 keV | Balloon experiments, NuSTAR in 2012 | Broad band imaging of all type objects |
| Lobster-eye (grazing incidence) | Few arcmin | 0.2–5 keV | Small payload prototypes | Wide Field monitoring and surveys |
| Laue Crystal Lens | ~1 to 2 arcmin | Few % variable in 0.1–1 MeV band | Balloon and laboratory experiments | Hard X-ray, soft gamma-ray spectroscopy, nuclear lines |
| Normal incidence reflection with ML coatings** | <1 arcsec (actual) | <0.25 keV ~1% bandwidth | Recent missions, for example, TRACE | Imaging soft X-ray lines in the solar corona |
| Diffractive-refractive | 10 to 100* microarcsec | >4 keV~ 10–20% bandwidth | Laboratory experiments | Central regions of galaxies + jets nearby stars |
| Interferometer | 0.1* microarcsec | 0.2 to 10 keV | Laboratory experiments | Imaging the environments of super massive black holes |

* Expected resolution. ** multilayer coatings. *** In 2010, the Chandra X-Ray Observatory, XMM-Newton, Suzaku, and Swift XRT Total telescope areas at 1 keV are, respectively, 0.09 $m^2$, 0.43 $m^2$ (3 tel), 0.18 $m^2$ (4 tel), and 0.015 $m^2$.

opaque to extragalactic sources along all directions and to sources in the galactic plane more distant than 200 parsec (650 light-years, $6 \times 10^{18}$ m). The upper limit has been determined in practice by the high-energy cutoff of grazing incidence optics. However, the employment of multilayer coatings plus longer focal lengths will extend the upper limit to nearly 80 keV starting with the launch of the NuSTAR mission, scheduled for 2012. Other papers in this issue describe how a structured array of Laue crystals will be able to concentrate hard X-rays and soft gamma-rays including some nuclear lines onto detectors with good energy resolution and low background.

The birth of X-ray astronomy, the initial discoveries, and even the work cited in the award of the 2002 Nobel Prize in physics to Riccardo Giacconi were all accomplished with mechanically collimated large area gas proportional counters. However, most of the progress of the past twenty-five years can be attributed to the large increase in detection sensitivity, positioning accuracy, high-resolution images, and spectra obtained with focusing telescopes. They have had a profound effect upon our understanding of stars, star formation, "normal" galaxies, active galaxies, clusters of galaxies, cosmology, and other aspects of astronomy. Focusing X-ray optics has also contributed greatly to our knowledge about the Sun and even provided some surprising results about comets and planets in our solar system. After nearly 30 years of observing gamma-ray bursts (GRBs) and debating their origin, a focusing X-ray telescope solved the mystery by providing precise positions of their longer lived X-ray afterglow that resulted in optical identifications and the knowledge that GRBs are extragalactic including some that are among the most distant and therefore the youngest objects ever detected in any band of the electromagnetic spectrum.

With IXO as the flagship, plans for future X-ray missions are centered upon focusing telescopes as highly sensitive imagers and concentrators for spectroscopy, polarimetry, and timing measurements. However, as shown by the RXTE, Swift BAT and INTEGRAL missions that are currently in orbit, very large area and very large field of view collimated or coded mask counters will continue to have important roles in fast X-ray timing measurements of intense sources, as all sky monitors of bursts and transient sources as well as surveying the hard X-ray sky.

Nearly all of the focusing telescopes that have observed sources more distant than the Sun have been based upon grazing incidence optics. The only other so far is a short observation of the Crab Nebula by a Laue crystal lens aboard a balloon [1]. The various types of focusing X-ray telescopes, which are in different stages of development, are listed in Table 1. The major international general user X-ray observatories will continue to be based upon grazing incidence optics indefinitely. The others are special purpose devices with a superior property for a limited range of objectives.

## 2. X-Ray Reflection and Resolution

Nearly all the telescopes to date that have been engaged in cosmic X-ray studies are based upon very low angle, that is, "grazing incidence" or "glancing angle" reflection. The reflective coatings are a very smooth, stable layer of a heavy metal, such as gold, platinum, or iridium, sometimes with a thin chromium sublayer bonding it to the substrate. In the absence of absorption edges the reflectivity of an elemental coating is high at small angles but declines slowly with angle up to its "critical angle" beyond which it drops precipitously. For a given X-ray energy the critical angle is determined by the decrement in the coating material's index of refraction with respect to vacuum. The decrement increases with density. The theoretical reflectivity of 30 nm of iridium, the thickness of the Chandra coatings, with an

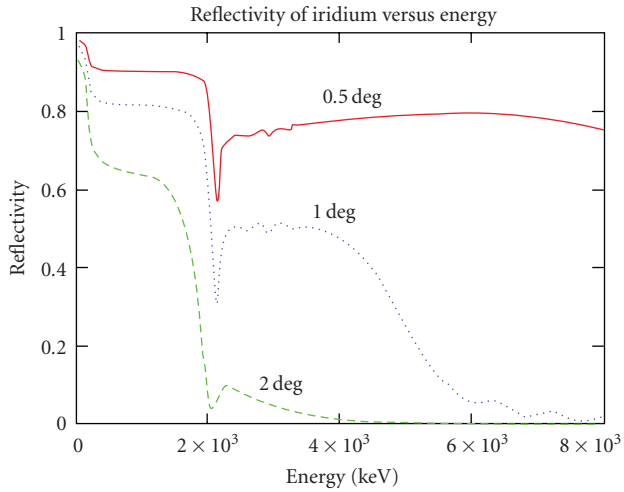


Figure 1: Reflectivity of 30 nm Iridium as a function of energy at three angles. The dips occur at the *M* absorption edges*.

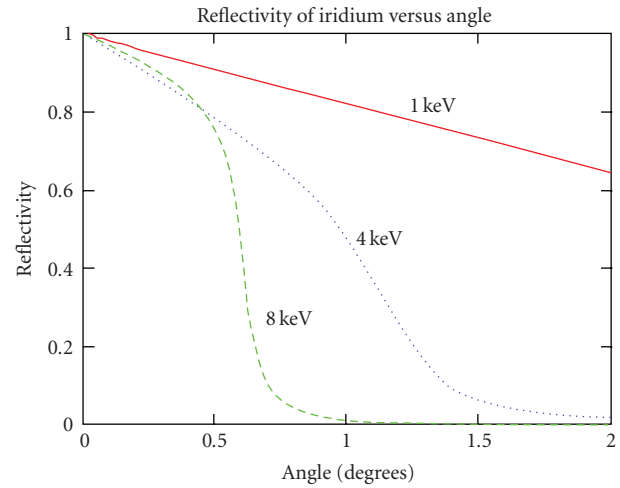


Figure 2: Reflectivity of 30 nm Iridium as a function of angle at three energies*.

rms surface roughness of 0.3 nm is shown as a function of angle for three energies and as a function of energy for three angles in Figures 1 and 2. (These results were obtained from the interactive CXRO web site of the Lawrence Berkley Laboratory, http://henke.lbl.gov/optical_constants/.) The abrupt changes in reflectivity that occur near 2 keV are due to iridium's M absorption edges. In the future this effect can be moderated but not totally eliminated by depositing a 10 nm carbon overcoat [2].

The point spread function (PSF), or resolution function of a grazing incidence telescope, consists of a core due mostly to local slope errors and a halo. The source of the halo is scattering by the irreducible small-scale surface roughness of the substrates and coatings. While smooth on the scale of visible light wavelengths the surface roughness of the most finely polished mirror is finite on the scale of X-ray wavelengths. Therefore the PSF is influenced by diffraction as well as by figure errors [9]. The fraction of photons in the halo increases with energy. The resolution is usually defined in the X-ray astronomy community as the diameter of the region that encompasses 50% of the total flux that accumulates with increasing angle and is called either the half power diameter (HPD) or the half energy width (HEW). Chandra's integral PSF on axis derived from a model that is based upon measurements at several energies in the large X-ray calibration facility at the Marshall Space Flight Center is shown in Figure 3. At 1 keV Chandra's on-axis HPD is about 0.5 arc seconds. At 9.7 keV Chandra's on-axis HPD is 1 arc second. With a Wolter 1 figure (Section 4.1) the angular resolution of the Chandra mirror degrades as the square of the angle off-axis. For example, at 8 arcminutes off-axis Chandra's HPD is 8 arcseconds at 1.5 keV. There is a more detailed description of grazing incidence X-ray reflection in a previous review by Aschenbach [10].

## 3. X-Ray Production in a Cosmic Setting

Many of the readers of this issue will have some degree of familiarity with X-ray detectors and optics but perhaps not with their astronomical applications. This section provides a brief description of several important objects in the X-ray sky that exemplify the broad range of topics that X-ray astronomy encompasses. More information about the science associated with X-ray astronomy can be found at several web sites including those of the following: Chandra X-Ray Observatory (http://cxc.harvard.edu/), NASA GSFC (http://imagine.gsfc.nasa.gov/docs/introduction/xray_information.html), Cambridge Institute of Astronomy (http://www-xray.ast.cam.ac.uk/xray_introduction/), and the 2nd edition of "Exploring the X-Ray Universe", F. D. Seward and P. Charles, Cambridge University Press, 2010.

The primary X-ray production processes include thermal radiation from a hot, that is, $\sim 10^6$ to $10^8$ degrees, plasma that consists largely of H and He ions plus small quantities, that is, $10^{-4}$ or less of the number of H atoms, of ions of C, O, Ne, Mg, Si, S, Fe, and so forth. Although their relative abundances are small, line emissions from highly ionized heavier elements are very prominent components of a thermal spectrum, especially at a temperature below 20 million degrees. By imaging the flux upon a position sensitive cryogenic detector with very high pulse height resolution and low background and/or imaging the output of a dispersive grating, focusing X-ray telescopes are an essential component of a high-resolution spectrometer.

Synchrotron radiation from high-energy electrons traversing a magnetic field and Compton scattering of longer wavelength electromagnetic radiation by high-energy electrons that results in higher-energy photons, commonly called "inverse Compton scattering", are two other primary X-ray production mechanisms. Other processes include bremsstrahlung and fluorescence radiation resulting from the impact of high-energy particles or higher-energy X-rays upon cold material or a warm plasma and charge exchange between ions and cold gases. Charge exchange from solar wind ions to the $H_2O$ and $CO_2$ in the halos of comets is the

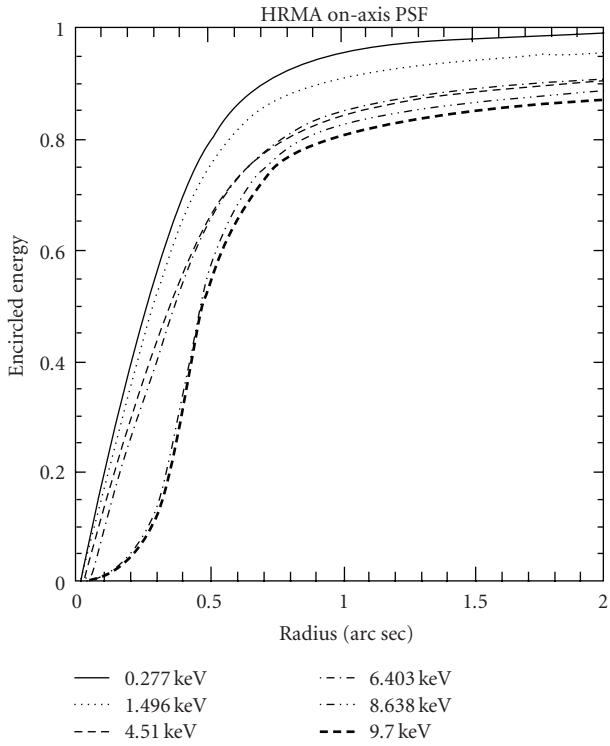


Figure 3: The integral point spread function of the Chandra X-ray telescope based upon measurements at several energies at the large MSFC X-ray calibration facility.

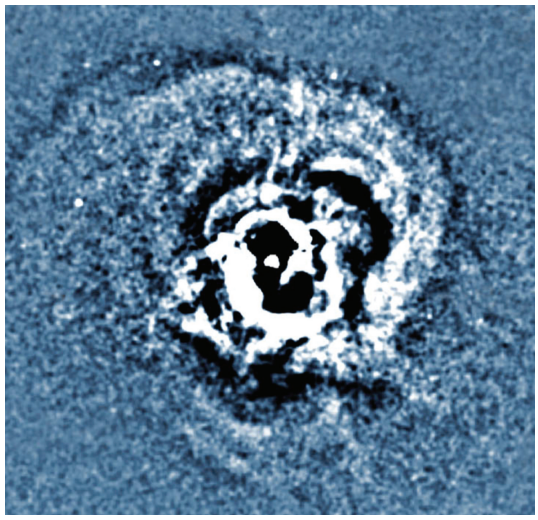

Figure 4: The Perseus cluster of galaxies has indications of episodic outbursts from the central galaxy, NGC 1275, very likely from the super massive black hole at its center. The size of the region is 400 arc seconds.

mechanism responsible for the surprisingly high-intensity and wide-spread X-ray emission from comets approaching the Sun.

There are environments where several processes are operating simultaneously. For example, the remnant of a young supernova remnant can emit thermal radiation as the

Figure 5: The Chandra X-ray image (pink) of the hot gas is superimposed on an optical image of two merging galaxies. The blue region shows the mass concentration as deduced from gravitational lensing. Field is 5.5 × 5.4 arc min.

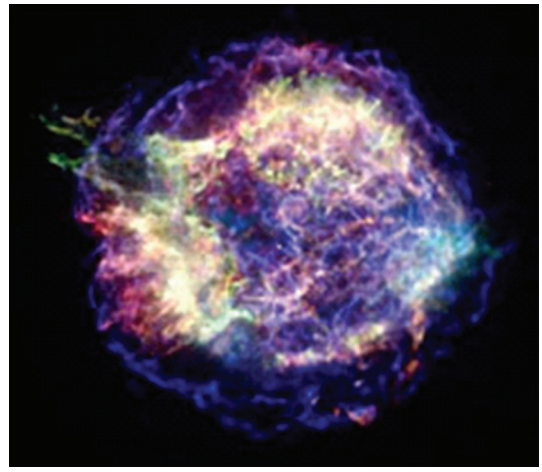

Figure 6: Chandra image of the over three-hundred-year-old supernova remnant, Cas A. The colors are "true" in that the higher energy X-rays are shown in blue and the lower energy X-rays in red. A point-like object near the center is not an ordinary star. It may be a neutron star remnant of a core collapse supernova explosion [3]. The size of the region is 7.3 × 6.4 arc minutes.

expanding ejecta collides with and shocks material in the interstellar medium or a shell of circumstellar matter shed during an earlier, milder eruptive phase in the life of the pre-supernova star. At the same time electrons may be accelerated to high energies by the shock waves and emit synchrotron radiation under the influence of a magnetic field.

The set of X-ray images that are shown illustrate the broad scope of X-ray astronomy. All images of cosmic X-rays sources were obtained by the Chandra X-Ray Observatory. They are available at http://chandra.harvard.edu/index.html. The principal sites of thermal radiation from hot plasmas include the hot gaseous medium within a cluster of galaxies. Figures 4 and 5 show two interesting examples of X-rays from galaxy clusters. While nearly all clusters of galaxies exhibit some structure or asymmetry in exposures with sufficiently high statistics, the very visible succession of waves shown in

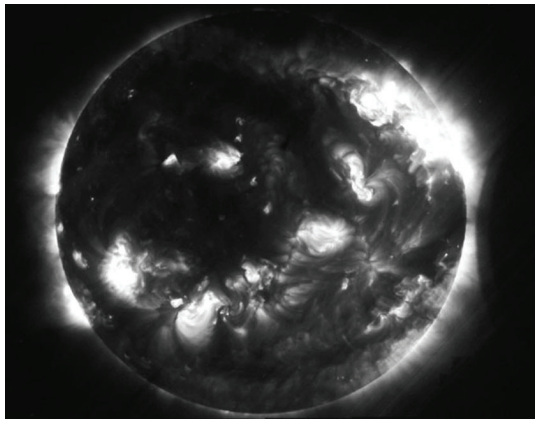

Figure 7: Image of the 6.35 nm $Fe^{16}$ line of the Sun's corona taken from a sounding rocket with a multilayer coated normal incidence telescope [4]. An edge of the Moon appears on the right near the time of an eclipse. Image was provided by Leon Golub of CfA.

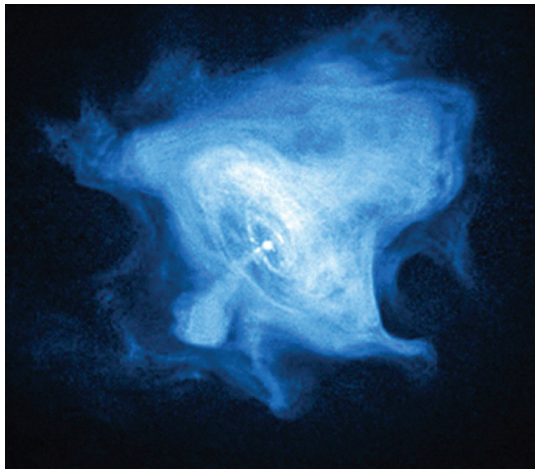

Figure 8: X-ray image of the Crab Nebula's neutron star pulsar and its wind nebula, which were created in a supernova explosion that occurred in 1054. They are near the center of the much larger optical image. The size of the region is 2.5 arc min.

Figure 4 is not typical of cluster emission but also not unique. They are evidence for a series of explosions emanating from the center of the central galaxy of the cluster, which houses a super massive black hole.

Figure 5 shows two clusters merging. The hot gaseous intracluster medium that each had contained (pink) previously has not yet settled into equilibrium with the new morphology of the gravitational field that was created by the merger. The mass concentration (blue) was determined by identifying gravitational lens effects. The significance of Figure 5 with respect to dark matter is discussed in Section 3.1. An X-ray image of a rich cluster of galaxies where the gas and galaxies have relaxed to an equilibrium state and are without an explosive center is an extended source of thermal emission from a relatively smooth distribution of hot (~50 million degrees) intracluster gas.

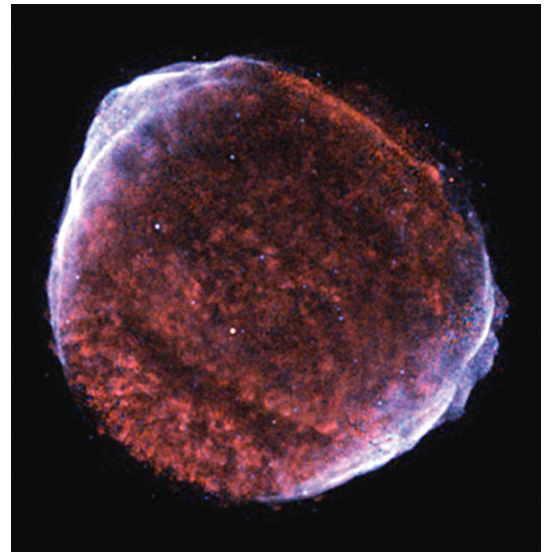

Figure 9: X-ray image of the remnant of a supernova that occurred in 1006. The spectrum of the blue regions at the perimeter is nonthermal and harder than the interior's and is believed to be sites of cosmic ray acceleration. The size of the image is 36 arc min.

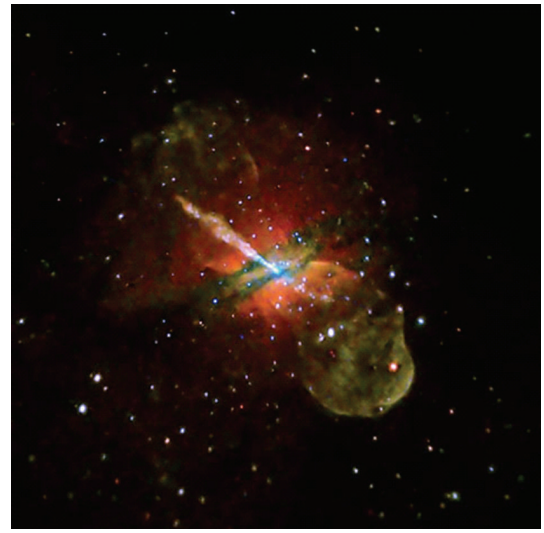

Figure 10: X-ray image of the radio galaxy Centaurus A. Opposing jets emanate from the center. The size of the image is 6.8 arc minutes.

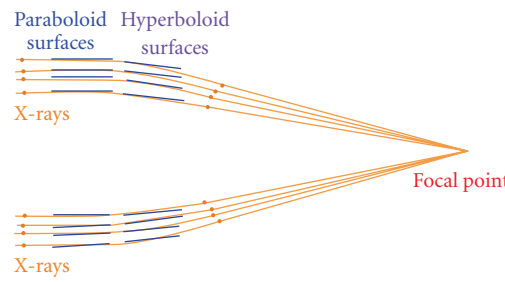


Figure 11: Focusing action of the Wolter 1 type grazing incidence telescope. Rays are reflected from the paraboloid to the hyperboloid and to the focus.

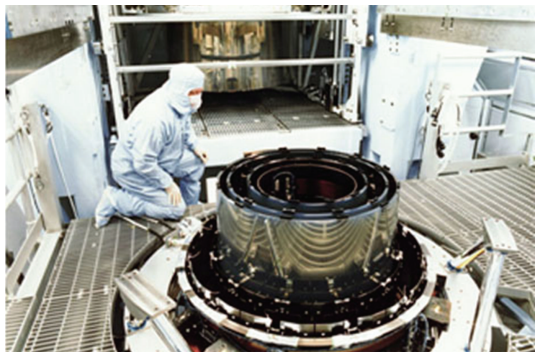

Figure 12: The Chandra telescope during integration of the four mirrors. The fourth mirror shell waits in the background.

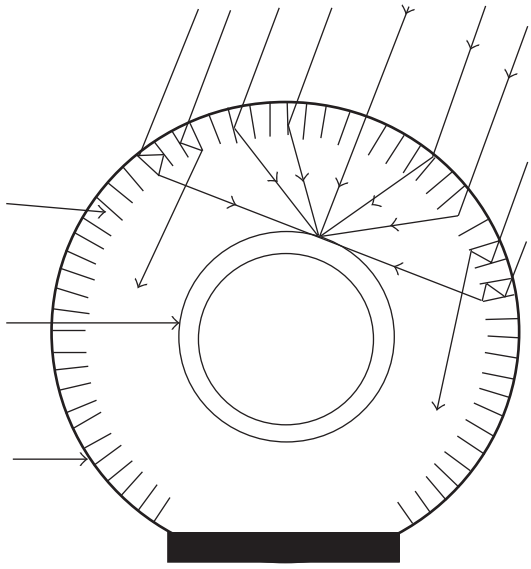

Figure 13: Lobster-eye optics are shown in one dimension. Except near the boundaries the focusing action is azimuthally symmetric. In the X-ray band the maximum graze angle is much smaller than shown in this sketch.

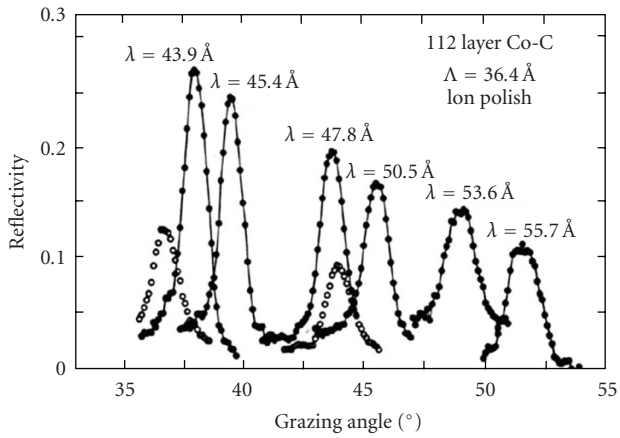


Figure 14: Soft X-ray reflectivity of a Co-C Multilayer coating [5, Figure 9.5].

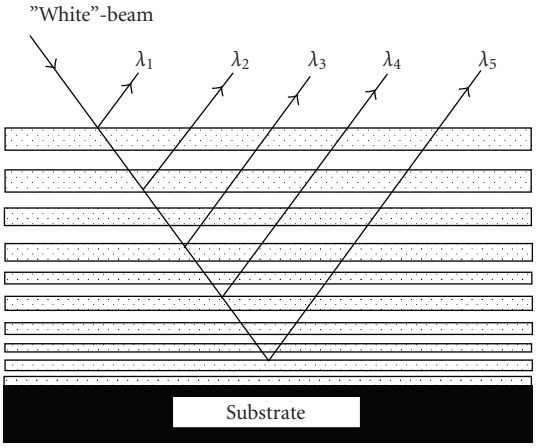


Figure 15: Reflection of hard X-rays by a multilayer whose period decreases with depth.

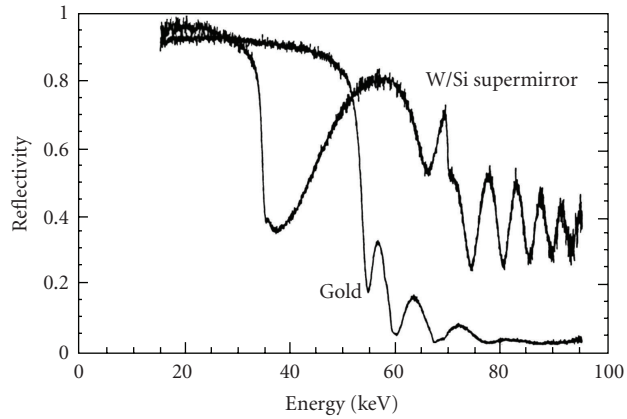


Figure 16: The observed X-ray reflectivities of gold and of a W/Si multilayer (oscillating line) at an angle of 3 mrad are shown [6].

The remnants of recent supernova explosions, Figure 6, are another source of thermal X-rays. Debris from the explosion expands and interacts with material from the interstellar medium. In many cases the supernova's environment is a circumstellar medium that was created when the pre-supernova star had experienced a previous, less disruptive mass ejection. In either case the surrounding medium is shocked by the rapidly expanding ejecta. In return, the ejecta themselves are shocked, that is, the "reverse shock", by the material it has encountered and add another, lower-temperature, thermal component to the total X-ray emission spectrum.

Thermal emission emanates from the few million degree coronas of the Sun (Figure 7) and stars. Stellar X-ray luminosities are only $10^{-11}$ to $10^{-7}$ that of the most luminous galactic X-ray sources. A base of more or less constant solar/stellar thermal X-ray emission underlies episodes of much higher-intensity transient nonthermal and thermal emission from dynamic active regions and flares. Thermal X-ray emission from plasmas with temperatures between 3 and 20 million degrees is characterized by very strong

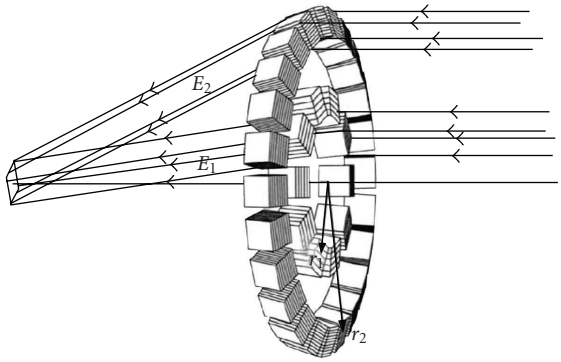


Figure 17: Laue crystal telescope illustrating that the energy that is concentrated varies with radius [7].

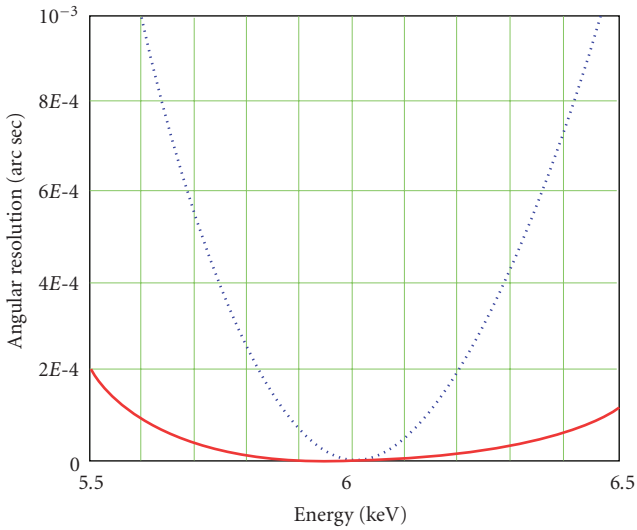


Figure 18: An example of the effect of chromatic aberration, in theory, upon the angular resolution of a diffractive-refractive pair is shown. The blue dotted line represents 1st order correction at 6 keV, the solid red line, correction to 2nd order [8].

emission lines from excitation and deexcitation of the heavier atoms. Both thermal and nonthermal processes account for the much higher than solar levels of X-ray emission and variability from members of star formation regions such as the Orion Nebula.

Rapidly rotating pulsars with high magnetic fields and their surrounding wind nebulae are sources of synchrotron X-ray radiation, the classic example being the Crab Nebula and its pulsar (Figure 8). Synchrotron X-rays are also a by-product of the acceleration of cosmic rays at the outer regions of expanding supernova remnant shells. A notable example of this process is the bright rims of SN 1006 (Figure 9).

Active galactic nuclei, that is, quasars, Seyfert galaxies, "BL Lac", and radio galaxies, are powered by accretion onto a super massive black hole (SMBH) at their centers. Figure 10 shows the relatively nearby radio galaxy Centaurus A, which is representative of many other radio galaxies. There is a central source at the SMBH and jets propagate outward from each side. Inverse Compton scattering is likely to be the mechanism responsible for the X-ray emission from the central source. Electrons are accelerated to high energy by mechanisms not thoroughly understood but probably involving the shock waves that are present. At the center the low-energy photon source for the inverse Compton scattering is the local environment of the accreting SMBH, such as a hot corona. There is no consensus on the mechanism powering the jets. According to Hardcastle et al. [11] and others the broadband spectral energy distribution and the X-ray spectrum imply a synchrotron origin for the X-rays. That would require electrons to be accelerated locally near the emission sites, not at the center. There is an alternative model based upon high-energy electrons experiencing inverse Compton scattering, the source of low-energy photons being the pervasive microwave background [12].

*3.1. Dark Matter and Dark Energy.* Observation of the X-ray emissions of clusters of galaxies has provided independent, corroborative evidence for the existence of dark matter and dark energy, two cosmological features that are not seen in fundamental particle experiments at accelerators. The indicator of dark matter is the presence of an extended, hot gaseous, X-ray emitting intracluster medium that pervades rich clusters of galaxies. Assuming that the galaxies have the same mass to light ratio as the Sun and nearby stars, the mass of the gas exceeds that of the visible portion of the galaxies significantly. However, the amount of mass that is needed to retain a gaseous halo with the observed temperature and spatial distribution is much greater than the mass of the gas. That proves that an additional component of mass exists, which is in fact the largest component. It is dark because it has not been seen in any band of the electromagnetic spectrum. The significance of Figure 5 is showing that the spatial distribution of the dark mass as inferred from gravitational lensing measurements is associated with the distribution of the galaxies, perhaps a surrounding dark halo, not the gas.

The existence of dark energy, which acts as a repulsive force that increases as the universe expands, is supported by two independent series of X-ray measurements. One is a standard candle approach based upon the premise that the gas-to-mass ratio in a rich cluster of galaxies is constant [13]. Its conclusion is in accordance with the earlier optical measurements that assume that type 1a supernova remnants are a standard candle. The other dark energy indicator is based upon observing the rate at which rich clusters of galaxies evolve. The evolution is influenced by a repulsive force that increases with time, which is the signature of dark energy [14].

## 4. Grazing Incidence Focusing X-Ray Telescopes

*4.1. Introduction.* The discovery of the first cosmic X-ray source occurred in 1962. That and the impressive amount of progress achieved in the subsequent 16 years, including the body of work that is cited in awarding the 2002 Nobel Prize in physics to Riccardo Giacconi, were all accomplished with

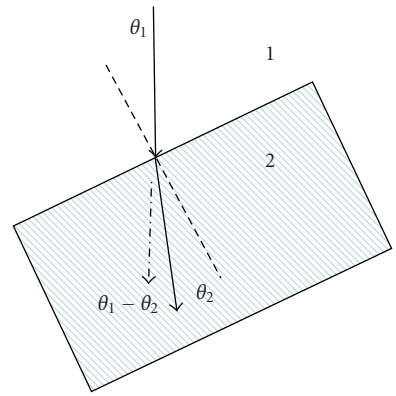


Figure 19: The left panel shows a ray (solid line) arriving at an interface between two media. The clear region "1" is a metal and the shaded region "2" is the vacuum, which has a larger index of refraction in the X-ray band. The dash-dot line is a continuation of the direction of the incident ray. We assume the interface should have been perpendicular to the incoming ray where it would have had no effect upon its direction. However, because of a slope error in the optic the interface is tilted at a finite angle of $\theta_1$. The angle of the refracted ray (dash-dot line) is $\theta_2$ so the error in the direction of the refracted ray is $\theta_1 - \theta_2$. Applying Snell's law relating the indices of refraction to the ray's directions the right panel calculates $\theta_2$. All angles are small so the angle and its Sin are essentially the same. The error is proportional to the difference in the indices of refraction. In the X-ray band the difference between beryllium and vacuum is of the order $10^{-6}$ to $10^{-5}$. Therefore the error is very small.

collimated gas proportional counters prior to the launch into orbit of the first focusing cosmic X-ray telescope. However, the potential power of focusing X-ray telescopes as a more sensitive and higher-resolution tool was recognized prior to all of those events in a 1960 paper by Giacconi and Rossi that described the increase in sensitivity that a parabolic concentrator would provide. In a paper appearing in a special issue of Experimental Astronomy, honoring the 400th anniversary of astronomical telescopes, Giacconi [15] reflects upon the history of the X-ray telescope from his unique perspective.

Although the focusing telescope concepts listed in Table 1 include several types, so far mostly one type, the grazing incidence telescope, has actually observed cosmic X-ray sources. The only exception is a brief balloon observation of the Crab Nebula with a Laue crystal telescope [1]. Furthermore, the figures of all of the grazing incidence telescopes that have been in orbit were fabricated in accordance with or approximating the Wolter1 geometry.

*4.2. Wolter Type 1 Telescopes.* Wolter [16] described several variations upon an imaging device consisting of two seemingly hollow cylinders in series with the diameter of each varying along the axis as a conic section curve. They were conceived as microscopes but the small dimensions and the high-resolution requirements made fabrication difficult and there are alternate approaches to X-ray microscopy [17]. However, the Wolter Type 1 geometry (Figure 11), sections of paraboloid and a hyperboloid in series, became the model for all of the cosmic X-ray telescopes that have been in orbit. Most of them consisted of several and in some cases many nested coaligned concentric Wolter 1 mirror pairs with a common focus.

The first Wolter 1 telescopes to be launched into orbit observed the Sun in 1973-1974 from the Apollo Telescope Mount (ATM) aboard the Skylab Space Station, the first mission to test the ability of humans to live and work in space for a substantial period of time. The Skylab ATM hosted two instruments, "S-O54" [18] and "S-O56" [19].

With a set of filters they recorded thousands of images on film over a period of nearly nine months. The film was returned to Earth by the Skylab astronauts.Van Speybroeck and Chase [20] provided a prescription for the Wolter 1 that high-resolution X-ray telescopes have followed or approximated. The high angular resolution telescope missions are the Einstein Observatory (1978–1981), ROSAT (1990–1999), and the Chandra X-Ray Observatory (launched in 1999), culminating in Chandra's 0.5 arc second resolution, half power diameter (HPD), on axis. In those three missions the optics consist of several, concentric integral, that is, full 360-degree cylinders, made of a thick, stiff, heavy material that can be accurately figured and finely polished without distortion. The Chandra telescope prior to final assembly is shown in Figure 12.

Wolter 1 telescopes with moderate or intermediate angular resolution and lower mass have been and are currently in space. Their optics have integral substrates, that is, whole cylinders, that are replicated from mandrels. The first of this type was EXOSAT (1983–1986) with epoxy-replicated Be backed mirror shells [21]. Next were electroformed nickel integral mirror shells [22]. This type of optic has achieved angular resolutions of 15 to 18 arc seconds and is probably capable of being improved. The first example was the focusing telescopes of the BeppoSAX mission (1996–2002). BeppoSAX obtained the first precise positions of gamma-ray bursts by imaging their X-ray afterglows. That led to identifying their optical counterpart and its extragalactic location [23]. At the beginning of 2010 the orbiting observatories with electroformed nickel telescopes are XMM-Newton (1999-) with three independent large area telescopes, each with 58 confocal parabola-hyperbola mirror shells and the much

smaller area single telescope Swift XRT (2004-) with 12 concentric mirror shells. The XRT, which Italy provided, is continuing the work of BeppoSAX by observing and accurately positioning the X-ray afterglows of gamma-ray bursts that are detected initially by the Swift Burst Alert Telescope, a large field of view position sensitive detector array with a coded aperture. Several of those positioned by the XRT are at cosmological distances. The XRT is addressing other objectives during the time between bursts that Swift detects at a rate of two per week. A new mission scheduled for launch in 2012 led by Russia includes an instrument named eRosita, being constructed in Germany, that contains a cluster of seven electroformed telescopes, each with 54 mirror shells. eRosita will extend the all-sky soft X-ray survey that was carried out by ROSAT to higher-energy X-rays. Many more AGNs are expected to appear because higher-energy X-rays will be able to penetrate the local absorbing matter surrounding a super massive black hole.

*4.2.1. Segmented Telescopes.* Lower angular resolution telescopes, specifically those built by the Goddard Space Flight Center for the Japanese ASCA (1993–2001) and Suzaku (2005-) missions, contained mirror shells made of much lighter, weaker aluminum foils that were segmented into several sections along the azimuth [24]. They approximated the parabola and hyperbola figures along the axis with straight lines; that is, they were double cones. Dipping the foils of ASCA in an acrylic lacquer solution under carefully controlled conditions followed by the deposition of a gold coating made their surfaces smooth and efficient X-ray reflectors. Because its substrates were flexible, the angular resolution of ASCA was about 3 arc minutes, limited by figure errors rather than the deviation of a double cone figure from the Wolter I paraboloid/hyperboloid. For Suzaku the foils were made smooth by an epoxy replication process that resulted in better than 2 arc minute resolution. Epoxy replication is also being used to coat the foils of telescopes for a future mission of the Japanese space agency [25]. Foil telescopes can accommodate a much higher packing density of mirror shells than the higher angular resolution telescopes and achieve a much better ratio of effective area to mass. They are well adapted for use with nondispersive spectrometer/detectors in the focal plane, such as solid state devices and (in the future) very high pulse height resolution cryogenic detectors. Foil mirrors are still an evolving technology [26].

Thermal forming of glass sheets whose thickness range is from 200 to 400 microns into telescope segments is another means of fabricating segmented X-ray telescopes [27, 28]. This technique is being used to manufacture the telescopes for the NuSTAR hard X-ray mission [29]. The thermal forming process is being refined at several institutions in the US and Europe for possible use in future missions including the International X-ray Observatory (IXO) [30–33].

Despite their angular resolution being relatively poor so far, segmented mirrors are the only practical option available to future very large area grazing incidence X-ray telescopes. The 3.3-meter diameter of the IXO telescope will be too large for the mirror shells to be integral structures. For the figure to be stable a complete cylinder of revolution with a 3.3-meter diameter would have to be very thick and therefore very massive. As described in other articles appearing in this issue in both Europe and the US there are currently major technology research projects devoted to improving the angular resolution of segmented mirrors for IXO. One approach is the aforementioned refinement of the process of thermal forming of glass segments. The other is assembling silicon mirror plates, known as "silicon pore optics" [34]. It is being developed under the supervision of ESTEC, the technology branch of ESA. While there is reason to expect significant improvement upon XMM-Newton, the 0.5 arc second angular resolution of the Chandra X-ray Observatory is not likely to be surpassed by any new grazing incidence telescope of its size or larger for a long time, if ever. Improvement upon Chandra on a significant scale will occur only with the development of a new technology.

In this issue, segmented optics are described in more detail in the article by Petre. A particular type of segmented X-ray telescope known as silicon pore optics is described in the article by Bavdaz et al.

*4.3. The Wide Field X-Ray Telescope (WFXT).* WFXT is a telescope concept that outwardly resembles the Wolter 1 but the figures of the front and rear sections are optimized polynomials instead of a parabola followed by a hyperbola. The field is "Wide" only in that the diameter where WFXT's angular resolution is less than 5 arc seconds is significantly larger than the Wolter 1's. The effective area as a function of angle off-axis is about the same for both. With polynomial figures the angular resolution of the telescope becomes much more uniform across the field of view and its average over the field of view is much superior to the Wolter 1. With current computer-controlled figuring and polishing techniques it is no more difficult to impart a polynomial figure to a mirror shell than a parabola or a hyperbola. Moreover, with the resolution not needing to be better than about 5 arc seconds it should be much less expensive to construct and less massive per unit area than the Chandra telescope. An early polynomial design was described by Burrows et al. [35]. Others have followed including a paper by Conconi and Compana [36]. The objective of WFXT is performing sensitive deep surveys that will discover and characterize extremely large populations of high redshift AGNs and observe the growth and development of clusters of galaxies. The WXFT concept and its scientific objectives are described in a "White Paper" [37] presented to the 2010 Decadal Astronomy Survey Committee of the US National Academies of Science.

*4.4. Kirkpatrick-Baez Telescopes.* Kirkpatrick and Baez [38] described a grazing incidence focusing device consisting of two orthogonal reflectors with each having the figure of a parabola in one dimension (KB). One-dimensional KB X-ray telescopes with several parabolic reflectors were constructed for sounding rocket experiments that scanned several older supernova remnants [39–41]. In a series of rocket flights

a 2D KB telescope imaged several clusters of galaxies [42]. A 2D KB telescope with a resolution of 35 arc seconds was constructed and tested as a prototype unit [43] for a large area modular array of telescopes that was selected as an "Attached Payload" on the International Space Station but the Attached Payload program was cancelled ultimately. A KB telescope has not been in orbit. However, it should be considered seriously as a candidate for the optics of IXO.

A KB telescope has certain advantages when the resolution requirement is not required to be better than several arc seconds. It is much less difficult and less costly to fabricate, especially with the availability of very thin, smooth, fairly flat glass from Schott AG. The thermal forming process used by X-ray that is being developed further in both the USA and Europe for possible use by IXO should apply very well to KB telescopes. In fact, the first use of heat slumping glass for X-ray telescopes was the construction of a KB telescope for the EUV/soft X-ray bands [44]. In addition the silicon pore optics technology being developed by ESA's ESTEC for IXO for a Wolter telescope is also applicable to the fabrication of KB telescopes [45]. A KB telescope can be divided conveniently into modules of almost any size. For each half of the telescope the figure of a reflector need be highly accurate in only one dimension. The alignment between the two orthogonal sections is not critical; so they can be made independently without experiencing much difficulty in the final assembly process. However, the optical axes of the KB modules have to be coaligned in direction very accurately. In contrast, front-rear section alignment is very critical in the Wolter 1 geometry but the coalignment of the optic axes is not as critical.

However, the KB geometry is inferior to the Wolter in the following respects. In part because the KB geometry is inherently a segmented telescope achieving very high angular resolution like that of the Chandra mirrors is not feasible. Up to about 10 arc minutes off axis, the theoretical angular resolution of the Wolter is superior. For small angles the off-axis resolution of the KB telescope varies linearly with angle whereas it varies as the square of the angle for the Wolter 1. At a fixed focal length the bandwidth of the Wolter mirror is larger because its two reflections occur in series whereas the two reflections of the KB are orthogonal. Consequently KB reflector graze angles are higher; so their reflectivity is generally lower at higher energies. On the other hand the aperture of a KB telescope is filled with a smaller number of reflectors and has therefore lower mass than a Wolter. However, the aperture efficiency of the KB geometry is less than the Wolter's because open area is lost due to the finite thickness of the reflectors in both dimensions. The loss occurs in just one dimension for the Wolter because the parabolic and hyperbolic sections of the telescope are aligned or, for electroformed telescopes, consist of a single continuous shell. This is a less important issue when the substrate material is very thin. The article by Hudec that appears in this issue discusses KB telescopes.

*4.5. The Lobster-Eye Telescope.* The lobster-eye telescope differs from all the others in that its area and resolution are essentially independent of angle. Its principal application is very broad sky surveying, monitoring, and positioning soft X-ray transient and variable sources including X-ray components of gamma-ray bursts, their X-ray afterglows, X-ray "flashes", and certain Type 2 supernovas as well as other known and any yet to be discovered soft X-ray time variable phenomena from random directions. Its function in the soft X-ray band would be similar to that of the coded mask BAT (Swift) in the hard X-ray band and that of Fermi in the gamma-ray band. As shown by the fortuitous discovery of a soft X-ray flare from a supernova while the Swift XRT was observing the X-ray afterglow of a gamma-ray burst [46] the variable soft X-ray sky contains sources that BAT and Fermi would not detect.

The concept for one dimension was introduced by Schmidt [47] and independently in a 2D geometry by Angel [48], who noting, its resemblance to crustacean eyes, gave it the memorable name. The geometry in one dimension is shown in Figure 13. A real instrument is unlikely to cover such a large angle.

This geometry is not suitable to imaging extended X-ray sources. Its intrinsic angular resolution is inferior to both Wolter and KB telescopes and its point response function is rather complex. It includes a considerable number of X-rays that are not reflected in either one or both dimensions. As a result nearly as much or more power appears in multiple side lobes as in the main image. A hybrid 1D lobster-eye plus an orthogonal 1D coded aperture concept was described by Gorenstein and Mauche [49]. The hybrid has significantly more area and greater bandwidth than the 2D optic but the background contained in a line is much higher than the background in a point-like image. A small 1D lobster-eye prototype was constructed by Gorenstein et al. [50] Hudec et al. [51] constructed both orthogonal 1-D halves of a small lobster-eye telescope. A very light weight 2-D lobster-eye telescope prototype was made from square channel plates by Fraser et al. [52] and is undergoing further development. Because the square cells are very small, the core angular resolution is potentially rather high although there will still be side lobes from rays that are not reflected or reflected more than once in either dimension.

Lobster-eye X-ray imaging systems are discussed in the article by Hudec in this issue.

*4.6. Multilayer Coatings: Normal Incidence X-Ray Telescopes and Hard X-Ray Telescopes.*

*4.6.1. Multilayer Coatings.* A multilayer coating consists of alternate layers of two materials with very different indices of refraction, that is, a heavy material and a light material. Examples of heavy materials used in multilayer coatings are cobalt, nickel, tungsten, and platinum. Low-density coating materials include carbon, boron carbide, and silicon. The virtuous property of multilayer coatings is that they reflect at angles of incidence larger than the critical angle of the densest materials. Spiller [5, Chapter 7] discusses multilayer structures and the equations governing their reflection properties. At every plane where there is an abrupt change

in the index of refraction, a fraction of the incoming beam is reflected. If the reflected beams from successive layers are in phase, the amplitude of the net-reflected beam is greatly enhanced. The action is very similar to that of a Bragg crystal but the wavelengths are longer. However, X-rays are still absorbed as usual by the materials; so the goal is to reflect the X-ray before it can be absorbed by the coating along its incoming and outgoing paths. The intensity of the reflected beam is less, considerably less, at very large angles of incidence than the incident beam. Multilayer coatings benefit focusing telescopes at both the low-energy and high-energy boundaries of the X-ray band. The reflectivity of a multilayer at angles much larger than the critical angle of grazing incidence is shown in Figure 14 [5, Figure 9.5].

On the low-energy end, that is, <0.25 keV they make normal incidence telescopes possible. At high energy grazing incidence telescopes with multilayer coatings can have significant effective area up to 80 keV, and even higher energy, under certain conditions, although with decreasing efficiency and smaller field of view.

Interface roughness is a much more critical factor in the reflection efficiency of a multilayer than of a single coating. It reduces the sharpness of the change in the index of refractions that exists at each boundary between the two materials. The result is lowering the reflection efficiency at each interface, which is particularly destructive because of the dependence upon coherence of reflection at several interfaces. Two factors influence the interface roughness. One is the physical roughness of the substrate. In most common deposition processes the substrate's roughness will propagate to every interface of the multilayer. The other factor is interdiffusion of the two materials. Both diminish the abruptness of the change in refractive index at the interface between the two materials and as a result diminish its contribution to the amplitude of the reflected rays.

#### *4.6.2. Normal Incidence Soft X-Ray Telescopes*

*Angular Resolution and Bandwidth.* With grazing angles of the order of a few degrees for each of two reflectors the physical area of the substrates of a grazing incidence telescope is the order of a hundred times larger than their projected area. Furthermore, the projected area of a Wolter mirror shell is a narrow annulus that occupies only a fraction of the aperture it encloses. Limited by the allowed mass and cost, the telescope will contain several or even many concentric Wolter pairs that have to be aligned coaxially to a common focus. In contrast the physical area of a normal incidence mirror and the projected area of the aperture are (almost) identical. Therefore a normal incidence telescope has comparatively very light weight. The amount of surface area that has to be machined and polished to an accurate figure is much smaller. There is no need to coalign multiple mirror shells. With those factors in its favor it is reasonable to expect that the angular resolution of a normal incidence telescope will be superior to that of a grazing incidence telescope and will be much less expensive. It should be possible to fabricate a normal incidence telescope that is diffraction limited with an angular resolution of a milliarcsecond or better while Chandra's half arc second resolution may be better than a large area grazing incidence telescope ever achieves.

However, normal incidence X-ray reflection occurs only with multilayer coatings with a constant period. The bandwidth is very small. The reflection efficiency is low and is significant only at very low energies. In fact, the Sun is the only target whose X-rays are currently being observed by a normal incidence telescope. Its three-million-degree thermal spectrum is populated with lines from highly ionized, C, O, Ne, Fe, and other ionic species whose intensity is enough to be imaged individually. Line intensities and their ratios are important plasma diagnostics. To image multiple solar lines a normal incidence telescope on the TRACE spacecraft is divided into several pie sectors, each coated according to a different multilayer prescription tuned to a specific line. A rotatable blocking aperture with an open pie section plus a detector that can accumulate and readout upon command allows the Sun to be imaged in several lines sequentially.

Figure 7 is an image of the 6.35 nm line of the solar corona taken by the Normal Incidence X-Ray Telescope (NIXT) from a sounding rocket in July 1991 near a time when the Sun was in total eclipse when viewed from the Big Island of Hawaii, Mexico, and Central America. The circular edge of the Moon can be seen at the right.

To counter the low efficiency for use in cosmic X-ray astronomy, Windt et al. [53] described a configuration consisting of an array of multiple normal incidence telescopes that can function either individually or in concert as an interferometer. They point out that the optics technology and manufacturing tools already exist. Normal incidence optics very similar to what they describe is being employed by the photolithography industry to image EUV patterns for the production of densely populated integrated circuits [54].

However, while normal incidence telescopes may be effective in a few observations involving very soft solar and stellar X-rays, their scope is very limited.

*4.6.3. High-Energy Telescopes.* Christensen et al. [55] showed that a multilayer coating consisting of alternate layers of a heavy and light material whose period decreases gradually with depth is able to reflect harder X-rays at angles significantly higher than its critical angle. The reflection mechanism is similar to what occurs in normal incidence reflection. However while the multilayer coatings of a normal incidence telescope have a uniform period and a very small bandwidth, the depth variable period of a hard X-ray multilayer reflector is effective over a broad bandwidth. A hard X-ray will penetrate the multilayer stack until it arrives at the depth where the Bragg condition is fulfilled sufficiently by a range of consecutive layers (Figure 15). There it will reflect with a significant fraction of the hard X-rays surviving absorption by the heavier material along the incoming and outgoing paths.

This method of broadening the bandwidth is not effective at low energies because the absorption is too strong.

Figure 16 is the reflectivity of a W/Si multilayer at an angle of incidence of 3.0 mrad as a function of energy and that of gold as measured in monochromatic X-ray beams at the European Synchrotron Radiation Facility [6]. In Figure 16 the reflectivity of gold begins to fall rapidly at 20 keV while the reflectivity of the multilayer which is declining at the critical angle resumes at higher energy when the coherent contribution of the multilayer becomes effective as the absorption diminishes. The reflectivity is significant up to the 68 keV K edge of tungsten. The oscillations in the reflectivity of the multilayer as a function of energy that is characteristic of monoenergetic X-rays are smoothed to a large extent in practice because the hard X-ray spectra of cosmic sources are generally continuous and the events are accumulated in energy channels of finite width. In addition a telescope is likely to contain multiple concentric reflectors with a range of graze angles, whose contribution in total also results in smoothing the effective area as a function of energy. However, small amplitude oscillations in effective area versus energy may still persist; so multilayer-coated telescopes require a much more detailed calibration than telescopes with single metal coatings.

Gold, platinum, and iridium have finite reflectivity at higher X-ray energies only for very small graze angles compared to multilayer coatings. The difference in effective area above 20 keV between Wolter telescopes with multiple mirror shells with gold (or platinum or iridium) and W/Si coatings is even larger than the impression given by Figure 16 because the mirrors at larger graze angles where gold does not reflect have more geometric area.

Several missions with multilayer-coated hard X-ray telescopes are in development or have been proposed that take advantage of the broader bandwidth. The first will be NuSTAR, a NASA Small Explorer mission with the Danish Technical University providing the multilayer coatings, that is scheduled for launch in 2012 (http://www.X-ray.caltech.edu/). The other missions are Astro-H of Japan (http://heasarc.gsfc.nasa.gov/docs/astroh/), a hard X-ray imaging/Polarimetry mission by Italy [56], and a hard X-ray telescope for the International X-Ray Observatory.

## 5. The Laue Crystal Telescope

At energies above 80 keV it becomes increasingly difficult and eventually impossible to focus X-rays by grazing reflection with any type of coating. However, the band from 150 keV to a few MeV includes both the continuum of AGN spectra and nuclear lines. The signals are faint and detector background per square centimeter is high. Bragg and Laue scattering are processes that can focus or more accurately concentrate very high-energy X-rays/gamma-rays onto a small area detector. The distinction between the two virtually vanishes at very high energies. Telescopes consisting of an array of mosaic crystals have been constructed to address this regime. The principal centers of activity are currently the University of Toulouse [7, 57] and the University of Ferrara [58, 59].

The orientation of each crystal is adjusted such that it diverts a narrow energy range of the incoming parallel beam to the focus. Each crystal is actually a mosaic of many smaller crystals whose orientation varies slightly. A gamma-ray entering the crystal will be reflected when it encounters a section of the crystal where the Bragg condition is fulfilled. The imperfections are beneficial because the mosaic arrangement of the crystallites results in a larger bandwidth.

The angular resolution of the optics is expected to be about an arc minute and the field of view, 5 to 10 arc minutes. Depending on the energy Laue crystal optics have longer focal lengths than grazing incidence optics. Therefore expandable optical benches or short distance formation flying between optics and detector are required. An international consortium has proposed to ESA to develop a major hard X-ray/gamma-ray mission based upon a Laue crystal telescope [60].

There was a successful balloon flight of this type of instrument, which detected soft gamma-rays from the Crab Nebula [1].

The paper entitled "Laue gamma-ray lenses for space astrophysics: status and prospects" by Frontera and Von Ballmoss that appears in this issue provides a more detailed description of this technique.

## 6. Diffractive and Refractive X-Ray Optics

*6.1. Limitations on the Angular Resolution of Grazing Incidence Telescopes.* Although Chandra's 0.5 arc second angular resolution is far short of its 1 keV diffraction limit of 14 milliarcseconds, it will be difficult for a sizable future generation grazing incidence X-ray telescope to improve upon it. The quantity of substrate area that was machined, polished, and iridium-coated for Chandra is about 250 times larger than its effective area, and this ratio would be about the same for a future high angular resolution grazing incidence telescope.

To avoid the intolerable problems of large mass and thicker substrates that larger integral mirror shells would require, the mirrors will almost certainly have to be segmented into smaller and thinner parts. While it reduces the telescope's mass, segmentation increases the number of substrates required to have the correct figure and be aligned. The only viable approach to better figure control is employing "active optics", which consists of attaching piezoelectric or other type controllers to the rear face of deformable substrates and working interactively to form the figure. This process is under study for the future Generation-X observatory, which has a resolution goal of 0.1 arc second [63]. Gen-X effective area goal is 50 $m^2$ at 1 keV, nearly three orders of magnitude larger than that of Chandra. This author's view is that larger size future grazing incidence telescopes will at best be able to achieve only a modest improvement upon Chandra's resolution. Significant improvement requires a technology that is not based upon grazing incidence optics. Normal incidence optics with multilayer coatings is an option that has been very successful in obtaining high-resolution X-ray images of the solar corona. However, as noted in Section 4.6.2 normal

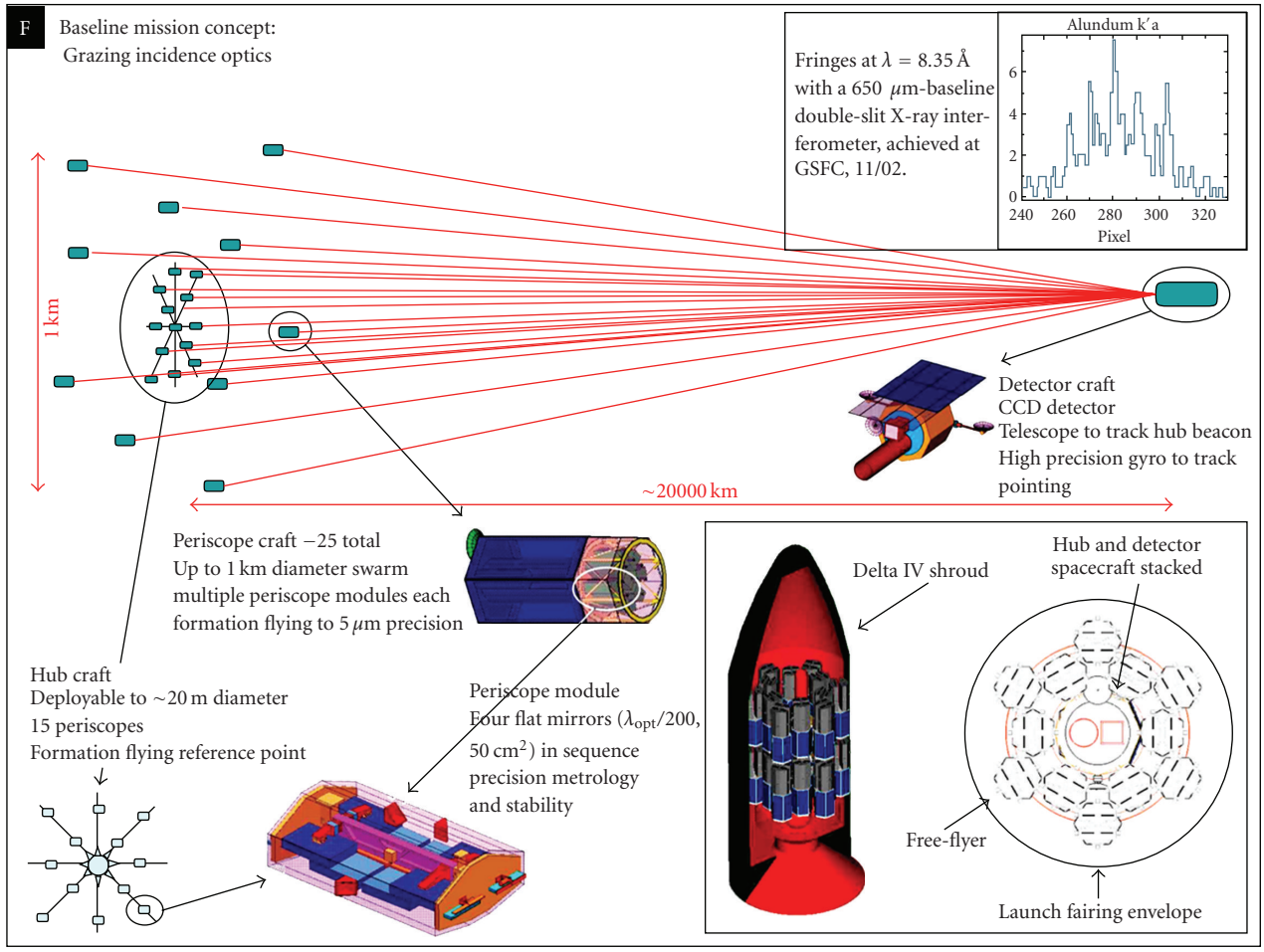


Figure 20: A possible configuration for an X-ray interferometer, Gendreau et al. [61]. In this example each of the collector optics are "periscopes" consisting of four grazing flat reflectors in series aligned such that the outgoing X-ray is insensitive to small angle rotations of the periscope [62].

incidence telescopes have low reflection efficiency and are effective only at long wavelengths and only over a very small bandwidth that must include a strong line to collect a sufficient number of photons. It is at best a special purpose device limited to imaging thermal X-ray lines with energies below one-quarter keV in nearby stars. Its scope is much too limited to be the technology for a future generation versatile high angular resolution cosmic X-ray observatory.

### 6.2. X-Ray Transmission: Diffraction and Refraction

*6.2.1. Introduction.* An alternative approach to higher angular resolution X-ray optics is based upon components that transmit rather than reflect X-rays. They include various levels of diffractive Fresnel zone plates (FZPs), which act as converging lenses, and refractive lenses [64], which can be either converging or diverging. Very small devices of both types are used routinely in experiments and microscopy at X-ray synchrotron radiation facilities. However with very intense, monochromatic beams at their disposal, laboratory scientists are not confronted with the problems of chromatic aberration, which is a characteristic of these devices. The sub-millimeter diameter of the laboratory devices frees them from the problems of very long focal lengths that are required by the meter and larger size components for astronomy.

Researchers at Tubingen University in Germany obtained images of the sun with very small Fresnel zone plates [65]. A few researchers have begun to consider diffractive-refractive optics as an option for high angular resolution X-ray astronomy [66–69]. However, a critical enabling technology, precision formation flying between widely separated spacecraft, does not yet exist. X-ray telescope missions will continue to be based exclusively upon grazing incidence optics as far one can foresee leaving ample time for better or worse to develop the formation flying capability and for the diffractive-refractive optics concepts to mature.

*6.2.2. Chromatic Aberration and Resolution.* The major issues for diffractive and refractive optics are that both are highly chromatic and that they have very low focusing power, resulting in the devices having extremely long focal lengths. The focal length of an FZP varies as the first power of

the energy, a lens as the second power. Skinner [66, 67] and at about the same time Van Speybroeck [70] in an unpublished memo described combinations of a FZP with an diverging refractive lens that correct chromatic aberration over a limited but significant range of bandwidth.

As described in the article by Skinner that appears in this issue, chromatic aberration can be corrected to first order when an optic consisting of a diffractive zone plate and a refractive lens is in direct contact. This occurs at the energy where the focal length of the lens is equal to minus twice that of the zone plate. That is the resolution and the first derivative of the combined focal length as a function of energy is zero. If the zone plate and lens are separated by the appropriate distance, a second-order correction can be achieved at a particular energy, that is, an energy where the resolution and its first and second derivatives as a function of the distance between the detector and optics are zero.

An example of the variation with energy of the resolution as a function of distance of the image from the optics is shown in Figure 18 for both cases. The average angular resolution as limited by chromatic aberration deteriorates as the bandwidth selected by utilizing the detector's energy resolution increases.

Figure 18 is a calculation of the contribution of chromatic aberration to the angular resolution of a diffractive-refractive pair whose focal lengths and separation satisfy the condition for a first-order correction (blue dotted line) and second order correction (red solid line). In both cases the prime energy is 6 keV and diffractive element is the basic Fresnel zone plate. For this calculation the diameter of the diffractive optic is 25 m and the focal length for the 1st order correction is 27,000 km. In the simulated 1st order correction the contribution of chromatic aberration to the resolution is less than 1 milliarcsecond from 5.7 to 6.5 keV. In the simulated 2nd order correction the contribution of chromatic aberration is less than 200 microarcseconds between 5.5 and 6.5 keV. However, the 2nd order system requires three spacecrafts to engage in precision formation flying and would not be considered until a later phase. The 6 keV diffraction limit as determined by the diameter of the components is not taken into account in Figure 17.

Transparency of the refractive lens is a major issue. It can be the most important factor driving the focal length to high values and it determines the lower limit on energy. The radius of curvature of the lens varies directly with the focal length. For a given diameter a larger radius of curvature results in a thinner lens. If a simple full body lens would be too opaque, its spherical or parabolic surface would be stepped back to a reference plane and become a Fresnel lens consisting of concentric zones, each zone with the same figure it had on the original parabolic surface. A refractive Fresnel lens configured like that made of a very light material such as beryllium can have very good transmission at 6 keV. If that is done for transparency without paying attention to maintaining phase coherence, each ring is essentially an independent lens. Their intensities will add. rather than amplitudes The diffraction limit will then be determined by the average width of the zone rings rather than the full lens diameter.

For a metal lens there is a small loss of efficiency due to large angle Laue scattering by the crystal planes of the metal.

*6.2.3. Advantages of a Transmitting Optic.* The most obvious advantage of a transmitting optic is that the areas of the aperture and the substrate are equal. The mass of a transmitting optic is a factor of $10^2$ smaller than its grazing incidence counterpart. With essentially no depth other than a web of support structure for the FZP and lens, an optic (or several optics with different energy bands) can be stowed for launch and deployed in space. These favorable attributes are tempered by the fact that the product of the transmission and bandwidth is low. The efficiency of the simple zone plate with alternating open and closed zones is only 10% in the first-order image, with the rest being in the zero-order and fainter, higher-order images that mostly do not arrive at the detector. For comparison, the aperture efficiency of the 1.2 m diameter Chandra telescope is also only about 10%. As described by Skinner [66] FZPs with a surface that is contoured or blazed to maintain phase over the entire aperture can have much higher efficiency at several energy intervals within a limited range of bandwidth.

Figure errors have much more impact upon the resolution of reflective optics than upon that of refractive optics. If the local slope of a reflector has an error of $\theta$, the direction of the reflected ray will have an error of $2 \cdot \theta$. When the ray is refracted at the interface between two media, the error is much smaller especially if there is only a small difference between the two indices of refraction. In the X-ray band the index of refraction of all materials is less than the vacuum's by a very small quantity, $\delta$. It is shown in Appendix A that for small angles the relation between the slope error at the interface between the lens and vacuum, $\theta$, and the direction of the refracted ray is $\delta \cdot \sin(\theta)$. For a refractive lens made of beryllium the values of $\delta$ at X-ray energies range from $10^{-5}$ to $10^{-6}$.

Surface roughness has much less influence upon diffractive-refractive optics than it does upon grazing incidence optics. A surface roughness of 10 nm would be disastrous for the efficiency of grazing incidence reflection at X-ray energies. However, assuming that the effect of surface roughness of a transmitting optic is to vary the path length of an X-ray passing through the material, 10 nm variations in path length through beryllium will result in very small variations in the phase over the area of the incident beam. The coherence of a beam traversing the optic will not be disrupted significantly.

While the small difference in refractive indices between the optic and vacuum mitigates the effects of slope errors and surface roughness, it also results in focal lengths being extremely long. A refractive optic with a diameter of 1 m will have focal length of the order of $10^3$ kilometers. Grazing incidence optics cannot benefit from very long focal lengths. The projected area of a mirror substrate would diminish and its mass would become larger as the length of the substrates increases to mitigate the reduction in projected area.

With less sensitivity to slope errors and surface roughness plus a much higher ratio of effective area to physical area diffractive and refractive optics should be much less

expensive to construct and have lower mass than grazing incidence telescopes.

However, it should be noted that although the angular resolution of diffractive-refractive telescopes may be very superior to Chandra's and the effective area larger within the energy band that is corrected for chromatic aberration, the sensitivity may not be superior. The very long focal length results in pixels with a large physical size that is more susceptible to cosmic ray-induced background. Also the detector is so far removed from the optics that the space between them cannot be enclosed to exclude background from diffuse cosmic X-rays and other sources. In any formation flying configuration the detector requires a local collimator, which is not nearly as effective in excluding diffuse X-ray background as the complete cover that exists over the space between a grazing incidence optic and a detector that are aboard the same spacecraft.

Diffractive-refractive X-ray optics including correcting chromatic aberration are described in more detail in the article by Skinner that appears in this issue.

## 7. X-Ray Interferometry

An X-ray interferometer is the ultimate tool for high angular resolution X-ray measurements and most likely for all of astronomy. The possibility of X-ray interferometry was demonstrated by Cash et al. [71] who observed interference fringes in the laboratory. There are many potential applications for an X-ray telescope with super high angular resolution. The crowning achievement would be an image of the event horizon of a super massive black hole (SMBH). A mission concept named the Black Hole Imager and its technical requirements were submitted as two "White Papers" to the U. S. National Academy of Science's Decadal Review of Astronomy and Astrophysics. One described the scientific significance of observing SMBHs at the centers of active galaxies [72, 73]. The other discusses the technology that would have to be developed to enable the measurements [61].

The resolution required to image a SMBH in an nearby external galaxy is about 0.1 microarcseconds. A few microarcsecond resolution would suffice for imaging the relatively small SMBH at the center of our galaxy, Sgr A*. However, the absorption along the line of sight in the galactic plane to Sgr A* may obscure important features of the event horizon and corona. Furthermore, several SMBH images are needed to obtain a consistent picture that not influenced by anomalous local conditions that is may exist at a single object.

For the diffraction limit to be below 0.1 microarcsecond at 6 keV, the diameter of the optics would have to exceed 500 m. Of necessity the Black Hole Imager would be a sparse aperture telescope, that is, an array of optics aboard separate spacecraft whose total area fills only a small fraction of the aperture. The system would resemble that of the optical/UV Stellar Imager concept [74], which consists of 30 static elements across 500 m. In a study for the NASA Institute for Advanced Concepts, Cash [75] estimated that an X-ray interferometer system would require a few dozen spacecraft to obtain a suitable image. As an alternative fewer elements can be used with changes in their alignments that create new baselines. The major differences are that the 10 km Stellar Imager focal lengths are much shorter than the Black Hole Imager's and the resolution in the optical/UV band is 0.1 milliarcsecond as compared to 0.1 microarcsecond at the X-ray energies. Also, the X-ray array has to be more stable and their relative positions known more accurate.

One of the outstanding issues is what the individual X-ray focusing or concentrating collectors should be. Currently the baseline collector is a "periscope" consisting of four flats in a grazing incidence configuration [62]. This geometry acts like a thin lens in that a slight tilt in direction does not affect the ray's outgoing direction. Appendix B shows a possible configuration for an X-ray interferometer with periscope collectors. However, the periscopes are massive and suffer from the shortcomings of grazing incidence reflection, such as sensitivity to local slope errors of the flats. Diffractive-refractive collectors would be much lighter, less expensive, and less sensitive to slope errors. However, the effect of chromatic aberration would have to be evaluated. For observing interference fringes a certain level of chromatic aberration may be tolerable when the detector is a cryogenic device with an energy resolution of 2 to 3 eV capable of recording interference patterns in narrow energy bands. More simulation studies are required to understand all the issues that affect X-ray interferometry, including whether or not a grazing incidence periscope or a diffractive-refractive pair is suitable collector.

## 8. Prospects for the Future

*8.1. Current and Future X-Ray Missions with Focusing Telescopes.* In 2010 four spacecrafts with focusing X-ray telescopes are operating. They are the Chandra X-Ray Observatory, XMM-Newton, Suzaku, and the Swift XRT. All appear to be in good health and have ample reserves of consumables, and the number of proposals from scientists hoping to utilize their capabilities remains high. In fact, the rate of oversubscription for observing time on the Chandra X-ray Observatory has not diminished after eleven years of operation. We can expect all of them to continue operations for an indefinite period. The Japanese space agency may possibly end support for Suzaku when a mission currently under development, Astro-H, is launched in a few years.

Table 2 lists the new missions which feature focusing X-ray telescopes that are in development plus three that have significant support from the astrophysics community but have not been approved. Those that have nominal launch dates have been approved or are likely to be approved. GEMS (http://heasarc.gsfc.nasa.gov/docs/gems/) is an X-ray polarimetry mission that has been selected for flight by NASA with the tentative launch date of 2014. The focusing telescope acts as a concentrator rather than as an imager; the targets are mostly point sources. eRosita [76] is the core instrument on the Russian Spektrum-Roentgen-Gamma (SRG) mission which is scheduled for launch in late 2012. The science driver is the detection of 50–100 thousand

clusters of galaxies up to redshift $z \sim 1.3$ in order to study the large-scale structure in the Universe and test cosmological models including Dark Energy.

NHXM and WFXT are included in Table 2 while other mission concepts have not because these two concepts are recognized as potential missions by the Italian Space Agency as well as from a team of astrophysicists. NHXM [56] consists of four identical telescopes with multilayer coatings. Three of the four telescopes will have at their focus identical spectral-imaging cameras while the fourth will have an imaging X-ray polarimeter. Other small-and medium-scale X-ray telescope missions are likely to be proposed in response to future announcements of opportunity from the space agencies.

While its launch date is very far off, the Generation-X mission concept [63] was the subject of a NASA-funded study and is generally recognized internationally as the successor to IXO.

In addition there may be other missions such as EXIST (http://exist.gsfc.nasa.gov/) where a focusing X-ray telescope is an important adjunct, not a component of the principal instrument.

IXO is the flagship mission of the major space agencies. Except for Gen-X, which is in the concept definition, phase IXO is the only observatory class mission of this group. Its major distinguishing capability is high-resolution spectroscopy from 0.15 to 10 keV with very high collecting area plus a hard X-ray telescope to measure the continuum up to ~80 keV. While its angular resolution cannot match Chandra's, it will be better than XMM-Newton's and is the best of this group (if Gen-X is not included). While Chandra is providing a library of high-resolution X-ray images, neither it nor XMM-Newton has the spectroscopic resolution and throughput required for a quantitative or in some cases even a qualitative understanding of the astrophysical processes occurring in those environments. IXO will provide that spectroscopic capability.

IXO will have a grating spectrometer (http://constellation.gsfc.nasa.gov/technology/xgs.html) that disperses X-rays. The final configuration has not yet been determined. Both of the two concepts under consideration by limiting the range of azimuth covered by the gratings and dispersing orthogonal to the plane of reflection make the spectral resolution less sensitive to the PSF of the telescope [77].

*8.2. Developing New Technology for High Angular Resolution X-Ray Telescopes.* Except for Gen-X (http://www.cfa.harvard.edu/hea/genx/) the essential technologies required by the missions appearing in Table 2 already exist even if they have not yet reached the state of development that fulfills NASA's and ESA's highest "Technology Readiness Levels" (TRLs). They need support for the final effort required to meet those goals.

The areas that are essentially still in the concept phase and require major technical development include the grazing incidence active optics for the Generation-X observatory, diffractive-refractive imaging, and X-ray interferometry. It is not possible to provide launch dates for missions based upon those concepts.

Gen-X's angular resolution goal is 0.1 arcsecond on axis, a factor of five better than Chandra's on-axis resolution. NASA supported an initial concept study of the optics for Gen-X. Given the very large collecting area and the characteristic feature of grazing incidence optics that the physical area of the substrates is some hundred times later than their effective collecting area the techniques used to create the figure and polish the substrates of Chandra cannot be applied to Gen-X. Also, whereas each mirror of Chandra is two integral cylinders in series whose thickness increases with shell radius, the many larger radii mirrors for Gen-X will have to be segmented into multiple, light-weight parts to keep the mass under control and innovative methods of figure formation need to be developed. It is expected that meeting Gen-X's angular resolution goals will require active optics. That is, the substrates will be furnished with controllers that allow the figure to be controlled interactively both on the ground and in orbit.

In contrast to Gen-X, fabricating the optics for a diffractive-refractive imaging telescope should not be difficult. High-accuracy machining should be sufficient, although lithography may be needed to create small-scale features for blazing. The enabling technology that is lacking is not related directly to the optics or detectors; it is mission operations, long distance formation flying between two spacecrafts (or possibly three at a later stage) in particular. Only one of the spacecrafts can be in true orbit. The other (others) would have to be powered, most likely by ion engines to maintain their alignment. The target, the optics, and the detector have to be aligned along a common axis with an accuracy of a centimeter in the two lateral dimensions in order for the image to land on the detector. The distance between the optics and detector, which is relatively easy to determine, has a much larger margin. An efficient means of finding and changing targets has to be developed. One efficiency booster would be employing two detector spacecrafts. While one is observing, the other is proceeding to the next target position. Although NASA and ESA are studying systems for measuring the positions of widely separated spacecraft accurately for LISA, a general relativity experiment, they are not addressing the issue of aligning them accurately.

The very long focal lengths required by diffractive and refractive X-ray optics preclude laboratory testing and calibration of a full size system in X-rays. Testing will have to be performed with centimeter size models rather than with actual, meter size optics. Some tests may be performed with visible light. Also, because the concepts are relatively new, more simulation studies have to be performed to resolve issues like how to best increase the bandwidth while dealing with chromatic aberration and to what degree it is possible or desirable to blaze the components to maximize the throughput and resolution in certain energy bands possibly at the expense of others.

X-ray interferometry has the most technology issues to resolve, for example, defining the nature and method of fabrication of the collector optics, establishing and maintaining accurate alignment of up to some thirty spacecraft distributed over a kilometer, as well as formation flying

Table 2: Future missions with focusing X-ray telescopes.

| Mission or telescope | Agencies or countries | capabilities | Nominal launch date |
|---|---|---|---|
| International X-Ray Observatory (IXO) | NASA/ESA/JAXA | High-Resolution, High-Throughput X-ray Spectroscopy with Cryogenic Detectors and Dispersive GratingsSoft/Hard X-ray Imaging X-ray Polarimetry and Timing | 202? |
| NuSTAR | NASA | Hard X-ray Imaging | 2012 |
| eRosita (SRG) [76] | Germany/Russia | X-ray Survey | 2012 |
| Astro-H | Japan (JAXA) | X-ray Spectroscopy with Cryogenic DetectorHard X-Ray Imaging | 2013 |
| GEMS | NASA | X-Pay Polarimetry | 2014 |
| New Hard X-ray Mission (NHXM) | Italy (with collaborators) | Soft/Hard X-rayImaging X-Ray Polarimetry | To be determined |
| Wide Field X-ray Telescope (WXFT) | Italy/US | Cluster Evolution Medium Deep Survey | To be determined |
| Generation-X | NASA (funded study) | High angular resolution active optics, Very large collecting area, High Res. Spectroscopy, Polarization, and Timing. | Concept, Requires New Technology |

between all the optics spacecraft and a detector some $10^4$ km distant. A great deal of effort has to be applied to quantitative simulations of the performance. An X-ray interferometer and Stellar Imager have several issues in common including formation flying, maintaining the stability of a cluster of spacecraft, and reforming the configuration when the target position is changed. The common need should motivate the space agencies to proceed with the development of formation flying technology.

## Appendices

## A. Error in the Direction of a Refracted Ray

See Figure 19.

## B. Black Hole Imager/X-Ray Interferometer

See Figure 20.

## References


[1] P. Von Ballmoos, H. Halloin, J. Evrard et al., "CLAIRE: first light for a gamma-ray lens," *Experimental Astronomy*, vol. 20, no. 1–3, pp. 253–267, 2006.

[2] D. H. Lumb, F. E. Christensen, C. P. Jensen, and M. Krumrey, "Influence of a carbon over-coat on the X-ray reflectance of XEUS mirrors," *Optics Communications*, vol. 279, no. 1, pp. 101–105, 2007.

[3] G. G. Pavlov and G. J. M. Luna, "A dedicated chandra acis observation of the central compact object in the cassiopeia a supernova remnant," *Astrophysical Journal*, vol. 703, no. 1, pp. 910–921, 2009.

[4] L. Golub, "The solar X-ray corona," *Astrophysics and Space Science*, vol. 237, no. 1-2, pp. 33–48, 1996.

[5] E. Spiller, *Soft X-Ray Optics*, chapter 8, SPIE Press, Bellingham, Wash, USA, 1994.

[6] K. Joensen, "Discovery of a Central X-Ray Object in the Cygnus Loop," Ph.D. thesis, Physics Department, University of Copenhagen, 1995.

[7] J. Rousselle, P. von Ballmoos, N. Barrière et al., "High-Z crystals for gamma-ray optics," in *Optics for EUV, X-Ray, and Gamma-Ray Astronomy IV*, vol. 7437 of *Proceedings of SPIE*, August 2009, 74370L.

[8] P. Gorenstein, W. Cash, N. Gehrels et al., "The future of high angular resolution X-ray astronomy," in *Space Telescopes and Instrumentation 2008: Ultraviolet to Gamma Ray*, vol. 7011 of *Proceedings of SPIE*, 2008, 70110U.

[9] B. Aschenbach, "Boundary between geometric and wave optical treatment of X-ray mirrors," in *Optics for EUV, X-Ray, and Gamma-Ray Astronomy II*, vol. 5900 of *Proceedings of SPIE*, pp. 1–7, August 2005, 59000D.

[10] B. Aschenbach, "X-ray telescopes," *Reports on Progress in Physics*, vol. 48, no. 5, pp. 579–629, 1985.

[11] M. J. Hardcastle, R. P. Kraft, G. R. Sivakoff et al., "New results on particle acceleration in the Centaurus A jet and counterjet from a deep Chandra observation," *The Astrophysical Journal*, vol. 670, no. 2, pp. L81–L84, 2007.

[12] J. Kataoka and Ł. Stawarz, "X-ray emission properties of large-scale jets, hot spots, and lobes in active galactic nuclei," *Astrophysical Journal*, vol. 622, no. 2, pp. 797–810, 2005.

[13] S. W. Allen, D. A. Rapetti, R. W. Schmidt, H. Ebeling, R. G. Morris, and A. C. Fabian, "Improved constraints on dark energy from Chandra X-ray observations of the largest relaxed galaxy clusters," *Monthly Notices of the Royal Astronomical Society*, vol. 383, no. 3, pp. 879–896, 2008.

[14] A. Vikhlinin, A. V. Kravtsov, R. A. Burenin et al., "Chandra cluster cosmology project iii: cosmological parameter constraints," *The Astrophysical Journal*, vol. 692, no. 2, p. 1060, 2009.

[15] R. Giacconi, "History of X-ray telescopes and astronomy," *Experimental Astronomy*, vol. 25, no. 1–3, pp. 143–156, 2009.

[16] H. Wolter, "Spiegelsysteme streifenden Einfalls als abbildende Optiken für Röntgenstrahlen," *Annalen der Physik*, vol. 10, p. 94, 1952.

[17] A. G. Michette, "X-ray microscopy," *Reports on Progress in Physics*, vol. 51, no. 12, pp. 1525–1606, 1988.

[18] M. V. Zombeck, G. S. Vaiana, R. Haggerty, A. S. Krieger, J. K. Silk, and A. Timothy, "An atlas of soft X-ray images of the solar corona from SKYLAB," *Astrophysical Journal Supplement Series*, vol. 38, pp. 69–85, 1978.

[19] J. H. Underwood, J. E. Milligan, A. C. deLoach, and R. B. Hoover, "S056 X-ray telescope experiment on the Skylab Apollo Telescope Mount," *Applied Optics*, vol. 16, no. 4, pp. 858–869, 1977.

[20] L. P. Van Speybroeck and R. C. Chase, "Design parameters of paraboloid- hyperboloid telescopes for X-ray astronomy," *Applied Optics*, vol. 11, no. 2, pp. 440–445, 1972.

[21] B. C. Taylor, R. D. Andresen, A. Peacock, and R. Zobl, "The Exosat mission," *Space Science Reviews*, vol. 30, no. 1–4, pp. 479–494, 1981.

[22] O. Citterio, G. Bonelli, G. Conti, E. Mattaini, and B. Sacco, "High-throughput optics for X-ray astronomy (*)(**)," *Il Nuovo Cimento C*, vol. 13, no. 2, pp. 375–389, 1990.

[23] E. Costa, F. Frontera, J. Heise et al., "Discovery of an X-ray afterglow associated with the $\gamma$-ray burst of 28 February 1997," *Nature*, vol. 387, no. 6635, pp. 783–785, 1997.

[24] P. J. Serlemitsos, L. Jalota, Y. Soong, H. Kunieda, Y. Tawara, and Y. Tsusaka, "The X-ray telescope on board ASCA," *Publications of the Astronomical Society of Japan*, vol. 47, no. 1, pp. 105–114, 1995.

[25] A. Furuzawa, T. Miyazawa, K. Yasufumi et al., "The current status of the reflector production for ASTRO-H/HXT," in *Space Telescopes and Instrumentation 2010: Ultraviolet to Gamma Ray*, vol. 7732 of *Proceedings of SPIE*, 2010, 77323F.

[26] P. J. Serlemitsos, Y. Soong, T. Okajima, and D. J. Hahne, "Foil X-ray mirrors for astronomical observations: still an evolving technology," in *Space Telescopes and Instrumentation 2010: Ultraviolet to Gamma Ray*, vol. 7732 of *Proceedings of SPIE*, 2010, 77320A.

[27] C. J. Hailey, S. Abdali, F. E. Christensen et al., "Investigation of substrates and mounting techniques for the High Energy Focusing Telescope (HEFT)," in *EUV, X-Ray, and Gamma-Ray Instrumentation for Astronomy VIII*, vol. 3114 of *Proceedings of SPIE*, pp. 535–543, August 1997.

[28] M. A. Jimenez-Garate, C. J. Hailey, W. W. Craig, and F. E. Christensen, "Thermal forming of glass microsheets for X-ray telescope mirror segments," *Applied Optics*, vol. 42, no. 4, pp. 724–735, 2003.

[29] W. W. Zhang, "Manufacture of mirror glass substrates for the NUSTAR mission," in *Optics for EUV, X-Ray, and Gamma-Ray Astronomy IV*, vol. 7437 of *Proceedings of SPIE*, 2009, 74370N.

[30] C. J. Hailey, F. E. Christensen, W. W. Craig et al., "Overview of segmented glass optics development for the Constellation-X Hard X-ray Telescope," in *X-Ray and Gamma-Ray Telescopes and Instruments for Astronomy*, vol. 4851 of *Proceedings of SPIE*, pp. 519–527, August 2002.

[31] P. Friedrich, B. Aschenbach, C. Braig et al., "Manufacturing of Wolter-I mirror segments with slumped glass," in *Space Telescopes and Instrumentation II: Ultraviolet to Gamma Ray*, vol. 6266 of *Proceedings of SPIE*, 2006, 62661G.

[32] M. Ghigo, S. Basso, R. Canestrari, and L. Proserpio, "Development of hot slumping technique and last optical performances obtained on a 500 mm diameter slumped segment prototype for adaptive optics," in *Astronomical and Space Optical Systems*, vol. 7439 of *Proceedings of SPIE*, August 2009, 74390M.

[33] R. Hudec, V. Marsikova, M. Mika et al., "Advanced X-ray optics with si wafers and slumped glass," in *Optics for EUV, X-Ray, and Gamma-Ray Astronomy IV*, vol. 7437 of *Proceedings of SPIE*, August 2009, 74370S.

[34] M. J. Collon, R. Günther, M. Ackermann et al., "Stacking of silicon pore optics for IXO," in *Optics for EUV, X-Ray, and Gamma-Ray Astronomy IV*, vol. 7437 of *Proceedings of SPIE*, 2009, 74371A.

[35] C. J. Burrows, R. Burg, and R. Giacconi, "Optimal grazing incidence optics and its application to wide-field X-ray imaging," *Astrophysical Journal*, vol. 392, no. 2, pp. 760–765, 1992.

[36] P. Conconi and S. Campana, "Optimization of grazing incidence mirrors and its application to surveying X-ray telescopes," *Astronomy and Astrophysics*, vol. 372, no. 3, pp. 1088–1094, 2001.

[37] S. Murray and The WFXT Team, "Wide field X-ray telescope mission," White Paper, NAS Decadel Survey Committee on Astronomy, 2009, http://wfxt.pha.jhu.edu/documents/white-papers/WFXT_RFI.pdf.

[38] P. Kirkpatrick and A. V. Baez, "Formation of optical images by X-rays," *Journal of the Optical Society of America*, vol. 38, p. 766, 1948.

[39] P. Gorenstein, B. Harris, H. Gursky, R. Giacconi, R. Novick, and P. Vanden Bout, "X-ray structure of the Cygnus Loop," *Science*, vol. 172, no. 3981, pp. 369–372, 1971.

[40] S. Rappaport, W. Cash, R. Doxsey, G. Moore, and R. Borken, "Discovery of a Central X-Ray Object in the Cygnus Loop," *Astrophysical Journal Letters*, vol. 186, p. L15, 1973.

[41] M. C. Weisskopf, H. Helava, and R. S. Wolff, "An upper limit to an X-ray point source at the center of the Cygnus Loop," *Astrophysical Journal*, vol. 194, pp. L71–L74, 1974.

[42] P. Gorenstein, D. Fabricant, K. Topka, F. R. Harnden Jr., and W. H. Tucker, "Soft X-ray structure of the Perseus cluster of galaxies," *Astrophysical Journal*, vol. 224, pp. 718–723, 1978.

[43] D. Fabricant, L. Cohen, and P. Gorenstein, "X-ray performance of the LAMAR protoflight mirror," *Applied Optics*, vol. 27, no. 8, pp. 1456–1464, 1988.

[44] S. Labov, "Figured grazing incidence mirrors from reheated float glass," *Applied Optics*, vol. 27, no. 8, pp. 1465–1469, 1988.

[45] R. Willingale and F. Spaan, "The design, manufacture and predicted performance of kirkpatrick-baez silicon stacks for the international X-ray observatory or similar applications," in *Optics for EUV, X-Ray, and Gamma-Ray Astronomy IV*, vol. 7437 of *Proceedings of SPIE*, 2009, 74370B.

[46] A. M. Soderberg, E. Berger, K. L. Page et al., "An extremely luminous X-ray outburst at the birth of a supernova," *Nature*, vol. 453, no. 7194, pp. 469–474, 2008.

[47] W. K. H. Schmidt, "A proposed X-ray focusing device with wide field of view for use in X-ray astronomy," *Nuclear Instruments and Methods*, vol. 127, no. 2, pp. 285–292, 1975.

[48] J. R. P. Angel, "Lobster eyes as X-ray telescopes," *Astrophysical Journal*, vol. 233, pp. 364–373, 1979.

[49] P. Gorenstein and C. W. Mauche, "All sky high resolution cameras for hard and soft X-rays," in *High Energy Transients in Astrophysics*, S. Woosley, Ed., AIP Conference Proceedings, no. 115, p. 694, 1984.

[50] P. Gorenstein, E. Whitbeck, G. K. Austin et al., "Lobster-eye X-ray telescope prototype," in *Multilayer and Grazing Incidence X-Ray/EUV Optics III*, vol. 2805 of *Proceedings of SPIE*, pp. 74–80, August 1996.

[51] R. Hudec, A. Inneman, L. Pina, V. Hudcova, L. Sveda, and H. Ticha, "Lobster eye X-ray telescopes: recent progress,"

in *X-Ray and Gamma-Ray Telescopes and Instruments for Astronomy*, vol. 4851 of *Proceedings of SPIE*, pp. 578–586, 2003.

[52] G. W. Fraser, A. N. Brunton, N. P. Bannister et al., "Lobster-ISS: an imaging X-ray all-sky monitor for the International Space Station," in *X-Ray and Gamma-Ray Instrumentation for Astronomy XII*, vol. 4497 of *Proceedings of SPIE*, pp. 115–126, August 2002.

[53] D. L. Windt, S. M. Kahn, and G. E. Sommargren, "Concepts: X-ray telescopes with high angular resolution and high throughput," in *Hyperspectral Remote Sensing of the Land and Atmosphere*, vol. 4151 of *Proceedings of SPIE*, p. 441, 2003.

[54] C. Wagner and N. Harned, "EUV lithography: lithography gets extreme," *Nature Photonics*, vol. 4, no. 1, pp. 24–26, 2010.

[55] F. E. Christensen, A. Hornstrup, N. J. Westergaard, H. W. Schnopper, J. Wood, and K. Parker, "Graded d-spacing multilayer telescope for high-energy X-ray astronomy," in *Multilayer and Grazing Incidence X-Ray/EUV Optics*, vol. 1546 of *Proceedings of SPIE*, pp. 160–167, 1992.

[56] G. Pareschi, G. Tagliaferri, A. Argan et al., "The new hard X-ray mission," in *X-Ray Astronomy 2009; Present Status, Multi-Wavelength Approach and Future Perspectives: Proceedings of the International Conference*, vol. 1248 of *AIP Conference Proceedings*, pp. 567–576, 2009.

[57] P. Von Ballmoos, H. Halloin, G. Skinner et al., "Max—a gamma-ray lens for nuclear astrophysics," in *Optics for EUV, X-Ray, and Gamma-Ray Astronomy*, vol. 5168 of *Proceedings of SPIE*, pp. 482–491, August 2004.

[58] F. Frontera, A. Pisa, V. Carassiti et al., "Gamma-ray lens development status for a European gamma-ray imager," in *Space Telescopes and Instrumentation II: Ultraviolet to Gamma Ray*, vol. 6266 of *Proceedings of SPIE*, 2006, 626627.

[59] F. Frontera, G. Loffredo, A. Pisa et al., "Focusing of gamma-rays with Laue lenses: first results," in *Space Telescopes and Instrumentation 2008: Ultraviolet to Gamma Ray*, vol. 7011 of *Proceedings of SPIE*, 2008, 70111R.

[60] J. Knödlseder, "GRI: the gamma-ray imager mission," *Advances in Space Research*, vol. 40, no. 8, pp. 1263–1267, 2007.

[61] K. Gendreau, Z. Arzoumanian, W. Cash et al., "Black Hole Imager: What Happens at the Edge of a Black Hole?" 2009, http://maxim.gsfc.nasa.gov/documents/Astro2010/Gendreau_BHI.pdf.

[62] A. Shipley, W. Cash, K. Gendreau, and D. Gallagher, "Maxim interferometer tolerances and tradeoffs," in *X-Ray and Gamma-Ray Telescopes and Instruments for Astronomy*, vol. 4851 of *Proceedings of SPIE*, pp. 568–577, August 2002.

[63] R. Brissenden and The Gen-X Team, "Generation-X technology development program," White Paper, NAS Decadel Survey Committee on Astronomy, 2009, http://www.cfa.harvard.edu/hea/genx/media/papers/astro2010/Astro2010-Brissenden-Gen-X.pdf.

[64] A. Snigirev, V. Kohn, I. Snigireva, and B. Lengeler, "A compound refractive lens for focusing high-energy X-rays," *Nature*, vol. 384, no. 6604, pp. 49–51, 1996.

[65] G. Elwert, "X-ray picture of the sun taken with Fresnel zone plates," in *Structure and Development of Solar Active Regions*, K. O. Kiepenheuer, Ed., IAU Symposium, no. 35, p. 439, 1968.

[66] G. K. Skinner, "Diffractive/refractive optics for high energy astronomy. I. Gamma-ray phase Fresnel lenses," *Astronomy and Astrophysics*, vol. 375, no. 2, pp. 691–700, 2001.

[67] G. K. Skinner, "Diffractive-refractive optics for high energy astronomy II. Variations on the theme," *Astronomy and Astrophysics*, vol. 383, no. 1, pp. 352–359, 2002.

[68] P. Gorenstein, "Design, Fabrication, and Characterization of Multilayers for Broad-band, Hard X-ray Astrophysics Instrumentation," in *X-Ray and Gamma-Ray Telescopes and Instruments for Astronomy*, vol. 4851 of *Proceedings of SPIE*, p. 598, 2003.

[69] C. Braig and P. Predehl, "Efficient Fresnel X-ray optics made simple," *Applied Optics*, vol. 46, no. 14, pp. 2586–2599, 2007.

[70] L. P. Van Speybroeck, Internal CfA Memorandum, 2000.

[71] W. Cash, A. Shipley, S. Osterman, and M. Joy, "Laboratory detection of X-ray fringes with a grazing-incidence interferometer," *Nature*, vol. 407, no. 6801, pp. 160–162, 2000.

[72] K. C. Gendreau, W. C. Cash, A. F. Shipley, and N. White, "The MAXIM pathfinder X-ray interferometry mission," in *X-Ray and Gamma-Ray Telescopes and Instruments for Astronomy*, vol. 4851 of *Proceedings of SPIE*, pp. 353–364, August 2002.

[73] K. C. Gendreau, W. C. Cash, P. Gorenstein, D. L. Windt, P. Kaaret, and C. Reynolds, "MAXIM: the black hole imager," *Proc. SPIE*, vol. 5488, no. 3, p. 394, 2004.

[74] K. G. Carpenter, R. G. Lyon, C. Schrijver, M. Karovska, and D. Mozurkewich, "Direct UV/optical imaging of stellar surfaces: the Stellar Imager (SI) vision mission," in *UV/Optical/IR Space Telescopes: Innovative Technologies and Concepts III*, vol. 6687 of *Proceedings of SPIE*, August 2008, 66870G.

[75] W. Cash, "X-ray interferometry ultimate astronomical imaging," Final Report, NIAC, 2001, http://www.niac.usra.edu/files/studies/final_report/389Cash.pdf.

[76] P. Predehl, R. Andritschke, H. Böhringer et al., "EROSITA on SRG," in *Space Telescopes and Instrumentation 2010: Ultraviolet to Gamma Ray*, vol. 7732 of *Proceedings of SPIE*, 2010, 77320U.

[77] W. Cash, "X-ray optics: a technique for high resolution imaging," *Applied Optics*, vol. 26, pp. 2915–2920, 1987.